

Calculation of electron-energy-loss spectra of composites and self-similar structures

Iván O. Sosa, Carlos I. Mendoza, and Rubén G. Barrera

Instituto de Física, Universidad Nacional Autónoma de México, Apartado Postal 20-364, 01000 México, Distrito Federal, México

(Received 25 September 2000; published 19 March 2001)

We calculate electron-energy-loss spectra for self-similar systems of polarizable spheres using a previously developed theory for the electron-energy loss of a system of identical spheres. We do this by means of a recursive procedure and an effective “local” dielectric function, which contains, implicitly, the effects of spatial nonlocality due to correlations and multipolar interactions among the spheres, as well as some characteristics of the experimental setup. We also apply the procedure to systems of spheres with a continuum distribution of sizes. Finally, we propose a simple nonlocal generalization of Bruggeman’s differential effective medium theory.

DOI: 10.1103/PhysRevB.63.144201

PACS number(s): 71.45.Gm, 77.84.Lf, 82.80.Pv, 68.37.Lp

I. INTRODUCTION

Electron-energy-loss spectroscopy (EELS) has been a useful tool to study the dielectric response of materials in an energy region inaccessible to optical spectroscopies.¹ For example, the energy loss of electrons provided by a scanning transmission electron microscope has been used to determine the dielectric function of materials for energies up to around 60 eV.² In these experiments the valence electrons of the material are polarized by the impinging electrons, and this process provides energy-loss channels through the excitation of the collective electromagnetic modes of the system. From the theoretical point of view this process can be described using a dielectric approach. A formula that relates the electron-energy loss in a homogeneous system with the imaginary part of the inverse local dielectric function was first given by Bethe.³ There has been also an increasing interest in the use of EELS to study and characterize inhomogeneous systems, like interfaces, isolated and supported nanoparticles, and more recently, composites.^{4–9} Since the distinctive energy-loss peaks are associated with the excitation of electromagnetic modes, and the characteristic energy of these modes depends, among other things, on the geometry of the system, the energy-loss spectra provide information about its mesoscopic structure. For example, in the EELS experiments of Howie and Walsh (HW) on a composite consisting of an insulating matrix with metallic inclusions,^{8–10} the presence and identity of the metal was determined by the location, in the spectra, of the energy-loss peak corresponding to the bulk plasmon, while the location and structure of the energy-loss band at lower energies was associated with the excitation of interfacial or surface plasmons. Since effective-medium theories, which were successful to describe the optical properties of composites, proved to be inappropriate to interpret EELS spectra, HW proposed a phenomenological approach for the calculation of the energy-loss function. In this approach they introduce an effective local dielectric response whose parameters were determined with the help of an average over all possible electron trajectories.¹⁰ Later on, Barrera and Fuchs¹¹ (BF) were able to construct a more fundamental theory for the calculation of the energy loss for a granular composite through the introduction of an effective nonlocal (wave-vector dependent)

longitudinal dielectric response of the granular system. Alternative computational procedures have been also proposed, and the inclusion of retardation has been explored as well.¹⁵ Nevertheless, one of the distinctive features of the approach of BF is that through a wave-vector integration, they were also able¹² to derive an effective *local* dielectric response that could be used in Bethe’s formula to calculate the energy-loss function, as if the system were homogeneous. When the formula for this effective local dielectric response was compared with the phenomenological one proposed by Walsh and Howie, it unraveled all the approximations and considerations behind the HW phenomenological approach. One of the virtues of the formula for the effective *local* dielectric response derived from BF’s theory is that it contains, implicitly, the induced interaction among the spheres to all multipolar orders (in the mean-field approximation). This is the main difference between this expression and the ones derived by the effective-medium theories in the optical case, in which the induced interaction among the spheres is taken only to dipolar order. But having now an effective *local* dielectric function that takes into account the induced interaction to all multipolar orders, it is very tempting to try to apply some of the ideas behind the effective-medium theories, in the optical case, to the case of EELS.

In this paper we explore some of these ideas, in particular the ones developed by Fuchs and Ghosh on their study of the optical response of self-similar structures,¹³ and the ones of Bruggeman on his differential-effective-medium theory.¹⁴ More explicitly, we consider a system with a self-similar structure in which the size of the inclusions covers very different scales, each scale being much larger than the previous one. We also consider a polydispersed composite, that is, a composite with a given distribution of sizes. Then we apply a recursive procedure to calculate the effective *local* dielectric response of self-similar and polydispersed systems and compare the results for the energy-loss function for different selections of geometrical parameters. We also construct the composite by adding, at each step, infinitesimal amounts of the inclusions thus yielding a differential equation for the effective dielectric response, also known as differential effective medium theories (DEMT). The solutions of this differential equation are used to calculate the energy-loss function and the results are compared with the ones obtained

through the recursive method. The paper is organized as follows: In Sec. II we review very briefly the theory of BF and we discuss how the energy-loss probability function can be described in terms of an effective *local* dielectric response. The recursive procedure is introduced in Sec. III and the generalization of the DEMT is developed in Sec. IV. Finally, Sec. V is devoted to the discussion of our results and conclusions.

II. EFFECTIVE LOCAL DIELECTRIC FUNCTION

The objective of this section is to briefly review the construction of an effective local dielectric function that is directly related to the profile structure of the electron-energy-loss spectra. First, let us consider an unbounded system of $N \gg 1$ polarizable spheres of radius a located at random within an otherwise continuous matrix. The dielectric responses of the spheres and the matrix to an electromagnetic field oscillating at frequency ω are described by local dielectric functions $\varepsilon_1(\omega)$ and $\varepsilon_2(\omega)$, respectively. It is assumed that the system appears to be homogeneous at a length scale $l \gg a$, although it is highly inhomogeneous at a length scale of order a . This allows us to describe the process of energy loss by fast electrons traveling through the system in terms of an effective nonlocal dielectric function $\varepsilon_M(k, \omega)$. By nonlocal we mean a dielectric function that depends not only on the frequency ω of the electromagnetic field but also on its wave vector k . The wave vector dependence arises from correlations and multipolar interactions among the spheres induced by their finite size. It can be shown¹¹ that the probability per unit length, per unit energy, for an electron to scatter with energy-loss E , is given by

$$\frac{d^2 P(E)}{dl dE} = \left(a_0 \frac{m_0 v_I^2}{2} \right)^{-1} \Xi(E), \quad (1)$$

where a_0 is the Bohr radius, m_0 is the rest mass of the electron, and v_I is the speed of the incident electrons. The relation between the energy-loss probability density $\Xi(E)$ and $\varepsilon_M(k, \omega)$ is given by

$$\Xi(E) = \frac{1}{\pi} \int_{\omega/v_I}^{k_c} \text{Im} \left[- \frac{1}{\varepsilon_M(k, \omega)} \right] \frac{dk}{k}, \quad (2)$$

where k_c is an upper cutoff wave vector usually determined by the angular aperture of the electron-energy-loss detector.

It was also shown¹¹ that $1/\varepsilon_M(k, \omega)$ can always be written in the following spectral representation:

$$\frac{1}{\varepsilon_M(k, \omega)} = \frac{1}{\varepsilon_2} \left[1 + f \left(\frac{C_b}{u-1} + \sum_s \frac{C_s}{u-n_s} \right) \right], \quad (3)$$

where $f = \frac{4}{3} \pi a^3 N/V$ is the filling fraction of the spheres, $u = -1/(\varepsilon_1/\varepsilon_2 - 1)$ is the spectral variable and V is the total volume of the system. By spectral representation we mean that $1/\varepsilon_M$ can be written as a sum of terms with simple poles, and these poles are related to the excitation of the normal modes of the electric field within the system. For example,

the poles at $u=1$ and $u=n_s$ have strengths C_b and C_s , and correspond to the excitation of bulk and interfacial modes, respectively.

In the mean-field approximation the information about the geometry of the system is given by two statistical parameters:¹¹ the filling fraction f of spheres and their two-particle distribution function $\rho^{(2)}(r_{12})$, where r_{12} is the distance between the centers of two spheres. If one further assumes that the two-particle distribution function takes into account only the excluded-volume correlations, that is, $\rho^{(2)}(r_{12})=1$ for $r_{12} \geq 2a$ and 0 otherwise, it can be shown that the strengths of the modes C_b and C_s and the location n_s of the interfacial modes become functions of ka , and can be calculated from simple closed-form expressions.¹¹

Finally, the effective *local* dielectric function $\varepsilon_{eff}(\omega)$ is defined¹² through the expression

$$\frac{1}{\varepsilon_{eff}(\omega)} = W \int_{\omega/v_I}^{k_c} \frac{1}{\varepsilon_M(k, \omega)} \frac{dk}{k}, \quad (4)$$

where $1/W = \ln k_c v_I / \omega$. Note that the effective *local* dielectric function is not a property of the material only but also of the experimental setup through the parameters k_c and v_I . Using this definition one is now able to write

$$\pi \Xi(E) = \frac{1}{W} \text{Im} \left[- \frac{1}{\varepsilon_{eff}(\omega)} \right], \quad (5)$$

which looks formally identical to the formula first given by Bethe³ for the electron-energy-loss probability density through a homogeneous medium with dielectric response $\varepsilon_{eff}(\omega)$.

When the spectral representation of $1/\varepsilon_M(k, \omega)$, given in Eq. (3), is substituted into Eq. (4), one can show¹² that $1/\varepsilon_{eff}(\omega)$ has also a spectral representation given by

$$\frac{1}{\varepsilon_{eff}(\omega)} = \frac{A_{b_1}}{\varepsilon_1} + \frac{A_{b_2}}{\varepsilon_2} + \int_0^1 \frac{\mathcal{A}(n)}{n\varepsilon_1 + (1-n)\varepsilon_2} dn. \quad (6)$$

In this equation $1/\varepsilon_{eff}(\omega)$ is given as a sum of two discrete poles at $\varepsilon_1=0$ and $\varepsilon_2=0$, corresponding to the excitation of the bulk modes of the spheres and the matrix, respectively, plus an integral associated with the continuous distribution of the characteristic energy of the interfacial modes. Although $\varepsilon_{eff}(\omega)$ is a local dielectric function, the coefficients A_{b_1} , A_{b_2} , and $\mathcal{A}(n)$ contain all the information about the finite-size correlations and interactions among the spheres coming from $1/\varepsilon_M(k, \omega)$; explicit expressions for these coefficients can be found in Ref. 12.

A simple situation occurs when the resonant energies of the interfacial modes lie close together and the dissipation broadening contained in the imaginary part of ε_1 is large enough so they appear as a single peak in the energy-loss spectrum. In this case it is possible to approximate the infinite set of interfacial modes by a single-effective-surface mode. The strength and location of this effective-surface mode will be labeled A_σ and α_σ , respectively, and they are chosen as to satisfy the sum rules given in Ref. 12. In this approximation $\varepsilon_{eff}(\omega)$ is simply written as

$$\frac{1}{\varepsilon_{eff}(\omega)} \approx \frac{A_{b_1}}{\varepsilon_1} + \frac{A_{b_2}}{\varepsilon_2} + \frac{A_\sigma}{\alpha_\sigma \varepsilon_1 + (1 - \alpha_\sigma) \varepsilon_2}. \quad (7)$$

Put it in this form, Eq. (7) can be directly compared with the phenomenological model proposed by Howie and Walsh,¹⁰

$$\frac{1}{\varepsilon_{HW}(\omega)} = f \left[\frac{1}{\varepsilon_1} + g_{int} \left(\frac{3}{\varepsilon_1 + 2\varepsilon_2} - \frac{1}{\varepsilon_1} \right) \right] + (1-f) \left[\frac{1}{\varepsilon_2} + g_{ext} \left(\frac{3}{\varepsilon_1 + 2\varepsilon_2} - \frac{1}{\varepsilon_2} \right) \right], \quad (8)$$

where $g_{int} = 1/(1 + 3\omega a/v_1)$ and $g_{ext} = 2f/(1 + 2f)$ are phenomenological parameters that were estimated by an averaging procedure over electron trajectories. The comparison of Eqs. (7) and (8) shows that the expression given by Howie and Walsh for the dielectric response of an equivalent effective medium has exactly the same structure as the spectral representation of $\varepsilon_{eff}(\omega)$ in the single-surface-mode approximation. However, it can be shown¹² that their corresponding expressions for A_σ and α_σ in terms of g_{int} and g_{ext} are valid only in the $a \rightarrow 0$ and $f \rightarrow 0$ limits.

III. RECURSIVE PROCEDURE

The purpose of this section is to take advantage of the apparently local nature of the effective dielectric function $\varepsilon_{eff}(\omega)$, derived above, to construct the corresponding energy-loss response for systems with self-similar structures. Here we follow a recursive procedure similar to the one originally proposed by Fuchs and Ghosh¹³ within the context of the optical properties of self-similar composites.

In the first stage of the recursive procedure, a finite-volume fraction of component 1, Δf , is added to a second component 2, and the effective *local* dielectric function of the mixture is found. At the second stage, the same finite amount of volume fraction of component 1 is added to a host consisting of the effective *local* dielectric function of the first stage, and the effective *local* dielectric function of the mixture is found. This process is continued until the final overall volume fraction f of component 1 is reached. Since the effective *local* dielectric function, given by Eq. (4), contains information about the spatial nonlocality of the system, this procedure can be regarded as a nonlocal generalization of the method proposed by Fuchs and Ghosh¹³. This method assumes that the inclusions at each stage are large enough so the composite at the previous stage can be regarded as homogeneous.

The volume fraction f_i of spheres accumulated up to the i th stage, is

$$f_i = f_{i-1}(1 - \Delta f) + \Delta f, \quad (9)$$

where f_{i-1} is the volume fraction of spheres accumulated up to the $i-1$ stage. Continuing this process, after N iterations we obtain

$$f_N = f_0(1 - \Delta f)^N + 1 - (1 - \Delta f)^N. \quad (10)$$

Since the original host contains no spheres, $f_0 = 0$, then the overall filling fraction of spheres is

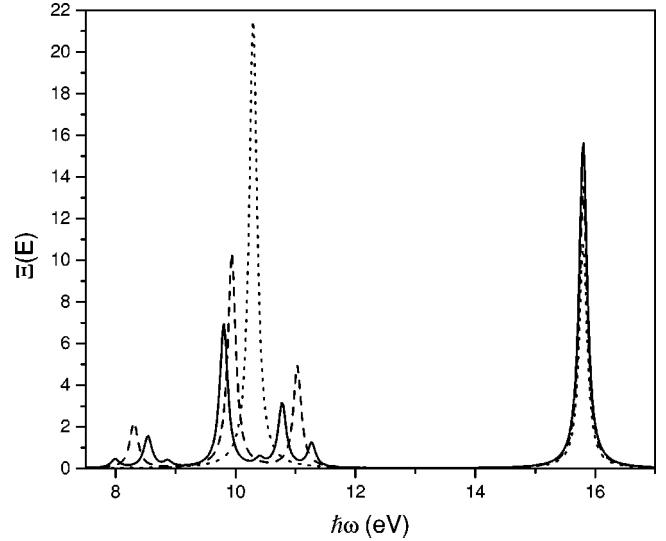


FIG. 1. Energy-loss probability function $\Xi(E)$ for a system of aluminum spheres in vacuum as a function of the energy loss $E = \hbar\omega$ for an overall filling fraction $f=0.15$, and Drude parameters for the aluminum $\hbar\omega_p=15.8$ eV, and $\omega_p\tau=100$. The dotted, dashed, and solid lines correspond to $N=1, 2$, and 3 recursive steps, respectively. The radius of the spheres is increased by a factor of 3 at each stage, starting with $a_1=2.5$ nm.

$$f = f_N = 1 - (1 - \Delta f)^N. \quad (11)$$

Therefore, for a recursive procedure of N stages, the volume fraction added at each stage is

$$\Delta f = 1 - (1 - f)^{1/N}. \quad (12)$$

Now we proceed to the calculation of the recursive procedure using the single-surface-mode approximation [Eq. (7)] for the effective *local* dielectric function at each stage. We present results for a composite made of aluminum spheres in vacuum. The dielectric response of aluminum is modeled by a Drude dielectric function $\varepsilon_1(\omega) = 1 - \omega_p^2/[\omega(\omega + i/\tau)]$, where ω_p is the plasma frequency and τ the relaxation time. In the results presented below, the plasma frequency of aluminum has been taken as $\hbar\omega_p = 15.8$ eV, and the relaxation time τ is used as a control parameter. Also, we have fixed $E_i = 100$ keV, which corresponds to the typical incident energies for electrons produced in a scanning transmission electron microscope, and the cut-off wave vector was taken as $k_c = 1.7 \text{ \AA}^{-1}$. In Fig. 1 we plot $\Xi(E)$ for systems with $N=1, 2$, and 3 recursive steps, $f=0.15$, and $\omega_p\tau=100$. The same amount of spheres were added at each stage using Eq. (12) and the radius of the spheres at stage i , a_i , is increased by a factor of three at each stage, starting with $a_1=2.5$ nm. We see that for stage 1 the curve for $\Xi(E)$ consists of two peaks, one close to $\hbar\omega \approx 10$ eV and the other at $\hbar\omega = 15.8$ eV. The first one arises from the interfacial modes and the second one corresponds to the bulk plasmon of Al. At stage 2, there are two new interfacial modes, and the original first-stage mode also appears but it is slightly shifted to lower energy and it has a reduced weight. At each subsequent stage, each of the newest modes

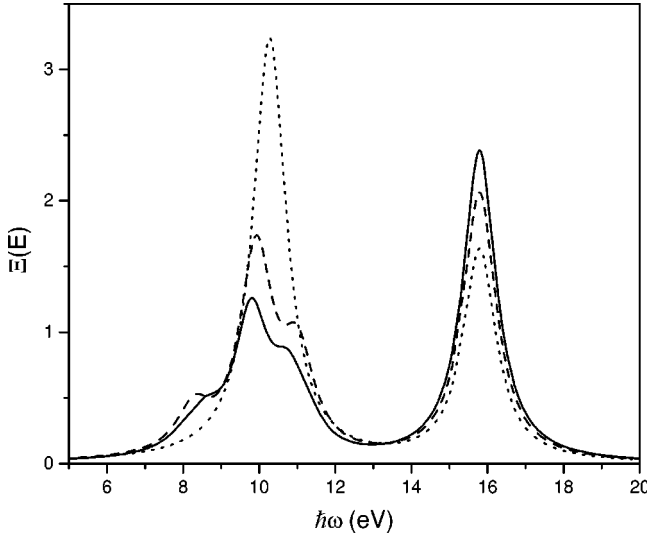


FIG. 2. The same as in Fig. 1 but with $\omega_p\tau = 15$.

of the previous stage yields two new modes, and all modes of the previous stages are still present, but with slightly different energies and with reduced weights. The peak corresponding to the bulk plasmon remains but with different weight. In Fig. 2, we use the experimental value for Al, $\omega_p\tau = 15$. Note that the behavior is the same as in Fig. 1 but the larger broadening of the peaks partially hides the peaks with small weights. The net result is a broad interface band with a rich profile.

We have stated that the size of the inclusions should increase at each successive stage in order for the composite of the previous stage could be regarded as a homogeneous effective medium. However, it is not clear to us how large this ratio of sizes, a_i/a_{i-1} , must be, or just how the theory breaks down when the size ratio is either close to 1 or even when it is less than 1. In Fig. 3 we explore the dependence of $\Xi(E)$ for different values of a_i/a_{i-1} . In panel (a) we plot $\Xi(E)$ for systems with $N=3$ recursive steps. The solid line corresponds to $a_i/a_{i-1}=2$, with $a_1=2.5$ nm. The dashed line corresponds to a fixed value for the radii of the spheres $a_1=a_2=a_3=5$ nm (which is the value of the radius for the spheres at the intermediate stage in the calculation of the solid curve). Panel (b) is the same as in (a) but for the solid line one takes $a_i/a_{i-1}=3$, with $a_1=2.5$ nm, and for the dashed one $a_1=a_2=a_3=7.5$ nm. Panel (c) is the same as (a) but with $N=5$ and the dashed line with $a_1=a_2=a_3=a_4=a_5=10$ nm. From these results one can see that the appearance of new interfacial modes at each iteration step should not be attributed to the increase of geometrical complexity of the system but rather to the recursive nature of the procedure itself. However, the exact energy and strength of the peaks does depend on the geometrical parameters of the system. Now, since the multipolar fluctuations in a system of identical spheres give rise to a collection of modes not present in the mean-field approximation, one concludes that the recursive procedure goes beyond the mean-field approximation, by taking into account, somehow, the multipolar fluctuations of the system. Similar conclusions have been already discussed, in the optical case, by Fuchs and Ghosh.¹³ Further-

more, we can see that even if the recursive procedure is not strictly valid whenever $a_i \approx a_{i-1}$, the use of fixed radii at all the stages together with the small (experimental) value of $\omega_p\tau$, does not change the results significantly. This suggests, that in this case, the role of the multipolar fluctuations is more relevant than having spheres with different sizes.

With these remarks in mind, we now apply the theory to a system of spheres with a continuum distribution of sizes. Let us denote by $D(a)$ the normalized distribution of radii of the spheres, for example, a log-normal distribution of sizes, that is,

$$D(a) = \frac{1}{\sqrt{2\pi a \ln \sigma}} \exp\left(-\frac{1}{2} \left[\frac{\ln(a/a_0)}{\ln \sigma}\right]^2\right), \quad (13)$$

where a is the radius of the spheres, a_0 is the mean radius, and σ is a measure of the width of the distribution, which is normalized to unity (see Fig. 4). In order to apply the recursive procedure, we divide the interval of sizes in a large number N of small intervals. Then we add the spheres recursively, as before, starting with the smaller spheres, with radius a_1 , up to the larger ones, with radius a_N . The spheres of the i th interval contribute to the overall filling fraction of spheres with the quantity

$$f(a_i) = D(a_i) f \Delta a, \quad (14)$$

where Δa is the width of the interval. The amount of spheres added at each stage, Δf_i , can be determined in the following way: For the larger spheres

$$f(a_N) = \Delta f_N, \quad (15)$$

then, for the immediately smaller ones

$$f(a_{N-1}) = \Delta f_{N-1} (1 - \Delta f_N), \quad (16)$$

and so on, so that

$$\Delta f_i = \frac{f(a_i)}{1 - f + \sum_{s=1}^i f(a_s)}, \quad (17)$$

where a_i is the radius of the spheres added in stage i .

In Fig. 5 we show the spectra of $\Xi(E)$ for systems with $N=30$ recursive steps, $f=0.15$, $a_0=2.5$ nm, and $\sigma = 1.1, 1.5$, and 2.5 . We see a broad peak corresponding to the interfacial modes and the peak due to the bulk plasmon. Note that the shape of the curves is essentially independent of the value of σ . Furthermore, the procedure converges rapidly with increasing N .

IV. GENERALIZATION OF THE DIFFERENTIAL EFFECTIVE MEDIUM THEORY

The DEMT is a differential recursive procedure in which, at each stage, the Maxwell Garnett theory (MGT) is used and an infinitesimal volume fraction of inclusions is added. The end result of this procedure is a differential equation for the effective dielectric function ϵ_M , whose solution is

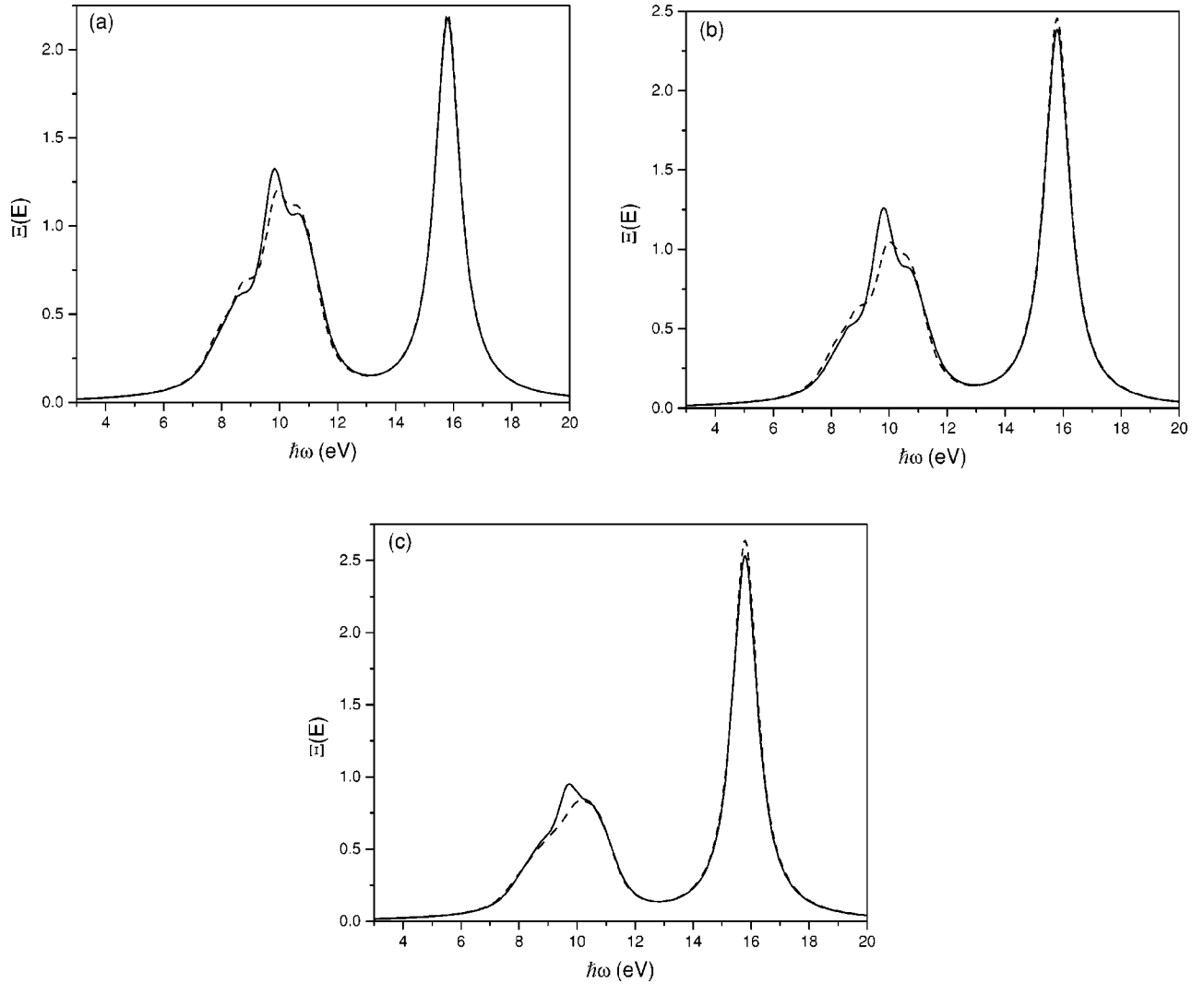


FIG. 3. (a) Energy-loss probability function $\Xi(E)$ for a system of aluminum spheres in vacuum as a function of the energy loss $E = \hbar\omega$ for an overall filling fraction $f=0.15$, and Drude parameters for the aluminum $\hbar\omega_p = 15.8$ eV, and $\omega_p\tau = 15$, and $N=3$ recursive steps. The solid line corresponds to a system with $a_i/a_{i-1}=2$, and $a_1=2.5$ nm (that is, $a=2.5, 5, 10$). The dashed line corresponds to a system of spheres with constant radius, $a=5$ nm. (b) The same as in (a) but the solid line here corresponds to a system with $a_i/a_{i-1}=3$, and $a_1=2.5$ nm (that is, $a=2.5, 7.5, 22.5$). The dashed line corresponds to a system of spheres with constant radius, $a=7.5$ nm. (c) The same as in (a) but with $N=5$ recursive steps. The solid line corresponds to a system with $a_i/a_{i-1}=2$ and $a_1=2.5$ nm (that is, $a=2.5, 5, 10, 20, 40$). The dashed line corresponds to a system of spheres with constant radius $a=10$ nm.

$$\left(\frac{\epsilon_M - \epsilon_1}{\epsilon_2 - \epsilon_1}\right)^3 = \frac{(1-f)^3 \epsilon_M}{\epsilon_2}. \quad (18)$$

It has been shown by Fuchs and Ghosh¹³ that the DEMA (Ref. 14) is a good approximation to the recursive MGT if the starting value of the filling fraction, in the recursive procedure, is small. Here we are going to generalize the DEMA to a system of spheres described by a nonlocal effective dielectric function. In order to keep the analysis as simple as possible we use a simplified version of the effective local dielectric response, due to Howie and Walsh,¹⁰ and given in Eq. (8).

In order to obtain an analytic solution of the problem, we are going to keep a constant through all the processes, which is valid as seen in the last section.

Let us add at each stage the same small amount Δf of inclusions. Thus, at the i th stage the filling fraction of spheres increases by

$$\delta f_i \equiv f_i - f_{i-1} = \Delta f(1 - f_i), \quad (19)$$

where we have used Eq. (9). Then the effective dielectric function at stage i can be written as

$$\epsilon_{HW}^{-1}(f_i + \delta f_i) = \epsilon_{HW}^{-1}[\epsilon_1, \epsilon_{HW}^{-1}(f_i), \Delta f]. \quad (20)$$

Using Eq. (8) we find

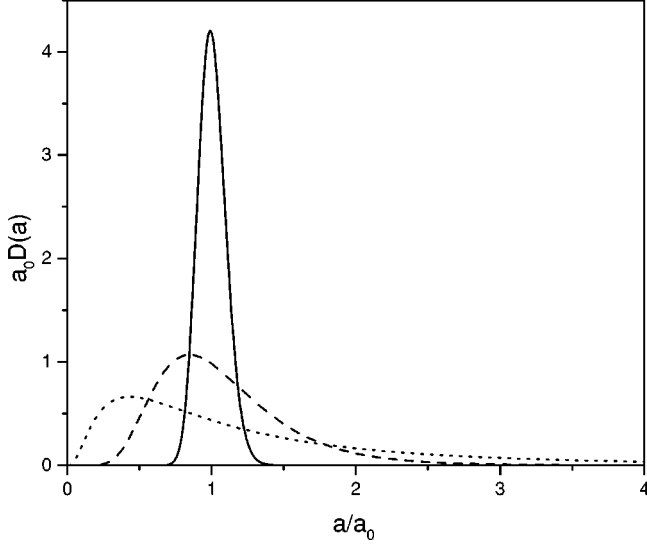


FIG. 4. $\tilde{D}(a)=a_0D(a)$ as a function of $x=a/a_0$ for three different values of $\sigma=1.1$ (solid), 1.5 (dashed), and 2.5 (dotted).

$$\begin{aligned} \varepsilon_{HW}^{-1}(f_i + \delta f_i) = \Delta f \varepsilon_1^{-1} & \left[1 + 2g_{int} \frac{\varepsilon_{HW}^{-1}(f_i) - \varepsilon_1^{-1}}{\varepsilon_{HW}^{-1}(f_i) + 2\varepsilon_1^{-1}} \right] \\ & + (1 - \Delta f) \varepsilon_{HW}^{-1}(f_i) \left[1 + \frac{2\Delta f}{1 + 2\Delta f} \right. \\ & \left. \times \left(\frac{\varepsilon_1^{-1} - \varepsilon_{HW}^{-1}(f_i)}{2\varepsilon_1^{-1} + \varepsilon_{HW}^{-1}(f_i)} \right) \right], \end{aligned} \quad (21)$$

where we used the definition of g_{ext} given below Eq. (8). Now, by expanding the above equation to first order in Δf ,

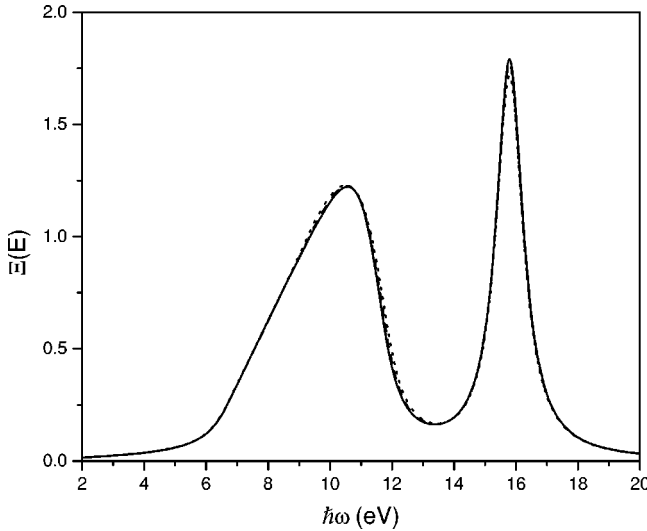


FIG. 5. Energy-loss probability function $\Xi(E)$ for a polydisperse system of aluminum spheres in vacuum as a function of the energy loss $E=\hbar\omega$ for systems with $N=50$ recursive steps, $f=0.15$, $a_0=2.5$ nm, Drude parameters for the aluminum $\hbar\omega_p=15.8$ eV, and $\omega_p\tau=15$, and $\sigma=1.1, 1.5$, and 2.5.

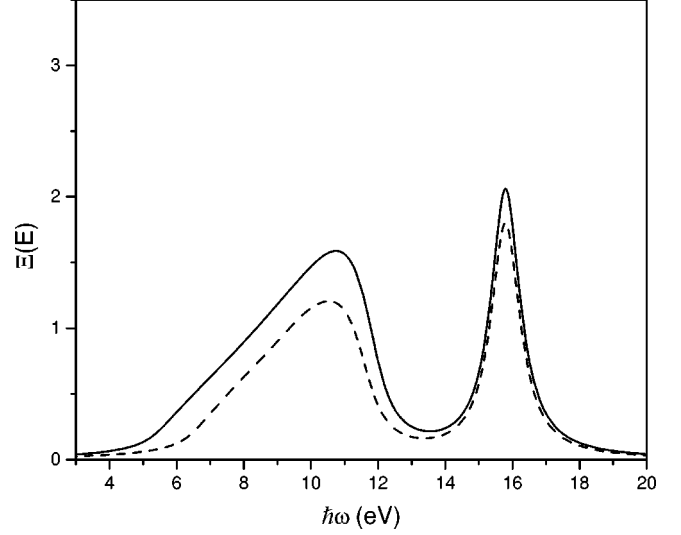


FIG. 6. Energy-loss probability function $\Xi(E)$ for a polydisperse system of aluminum spheres with $f=0.15$, Drude parameters for the aluminum $\hbar\omega_p=15.8$ eV, and $\omega_p\tau=15$, and $a=2.5$ nm. The solid curve corresponds to the nonlocal generalization of the DMT and the dashed curve corresponds to the recursive procedure with $N=15$ recursive steps and constant radius $a=2.5$ nm.

using Eq. (19), and taking the limit $\delta f_i \rightarrow 0$, one can show that Eq. (21) can be written as the following integral equation:

$$\begin{aligned} \int_{\varepsilon_2^{-1}}^{\varepsilon_{HW}^{-1}} \frac{[\varepsilon_{HW}^{-1}(f) + 2\varepsilon_1^{-1}] d\varepsilon_{HW}^{-1}}{[\varepsilon_{HW}^{-1}(f) - \varepsilon_1^{-1}][2g_{int}\varepsilon_1^{-1} - 3\varepsilon_{HW}^{-1}(f) - 2\varepsilon_1^{-1}]} \\ = \int_0^f \frac{df}{1-f}, \end{aligned} \quad (22)$$

which can be solved analytically, to get

$$\begin{aligned} \left[\frac{\varepsilon_{HW}^{-1}(f) - \varepsilon_1^{-1}}{\varepsilon_2^{-1} - \varepsilon_1^{-1}} \right]^9 \left[\frac{3\varepsilon_{HW}^{-1}(f) - 2(g_{int} - 1)\varepsilon_1^{-1}}{3\varepsilon_2^{-1} - 2(g_{int} - 1)\varepsilon_1^{-1}} \right]^{-2(g_{int} + 2)} \\ = \left(\frac{1}{1-f} \right)^{3(g_{int} - 5)}. \end{aligned} \quad (23)$$

This equation can be regarded as a nonlocal generalization of the DMT. We have also checked that the results given by Eq. (23) are equivalent to the ones obtained through the recursive procedure described in the last section, if we use the HW effective dielectric response, keep constant the radii of the spheres, and iterate till convergence is reached. In the case of a more accurate effective *local* dielectric response, like the one given in Eq. (4), the equivalence between the recursive procedure and the corresponding differential equation should also hold. Nevertheless, in this more general case an analytical solution of the differential equation might not be either possible or useful. In Fig. 6 we plot $\Xi(E)$ for a system of spheres with $f=0.15$, $a=2.5$ nm, using the nonlocal generalization of the DMT given by Eq. (23), and we compare it with the results obtained using the recursive procedure, as described above, but with the effective *local* di-

electric response given by the single-mode approximation [Eq. (7)]. As expected, the overall shape of both curves is similar, although the quantitative difference between them obviously comes from the use of different effective *local* dielectric responses.

V. CONCLUSIONS

We have constructed recursive procedures to calculate electron-energy-loss spectra of self-similar structures of polarizable spheres including the effects of spatial nonlocality arising from the correlations and multipolar interactions among the inclusions. These structures were constructed by adding larger and larger spheres at each stage. We found that at each iteration new peaks appear in the band of interfacial modes yielding spectra with a very rich structure. We also found that at each stage of iteration the peak corresponding to the excitation of the bulk mode changes its strength without shifting its energy; this is because the bulk mode is independent of the geometry of the system. We have also shown that the results obtained for self-similar systems of spheres can be well approximated by setting, in the recursive procedure, a constant radius around the mean of the ones in the self-similar structure and a wide enough broadening. Fur-

thermore, the recursive procedure was also applied to systems of spheres with a continuum distribution of radii. We found that the results for a log-normal distribution, with the same mean radius, were quite independent of the width of the distribution. All these results show that the appearance of new peaks at each iteration step in the recursive procedure is due to the generation of new modes whose physical origin is not the increasing complexity of the geometrical structure of the system but rather the account of multipolar fluctuations beyond the mean-field approximation. However, the exact energy and strength of the peaks do depend on the geometrical parameters of the system. Finally, we derived a simple nonlocal generalization of the DMT and showed its equivalence to the recursive procedure with an “infinitesimal” starting value of the filling fraction of inclusions.

ACKNOWLEDGMENTS

We acknowledge very illuminating discussions with R. Fuchs and the partial financial support of Dirección General de Asuntos del Personal Académico of Universidad Nacional Autónoma de México, through Grant No. IN-104297, and from Consejo Nacional de Ciencia y Tecnología (México) through Grant No. 27646-E.

¹See, for example, R. F. Egerton, *Electron Energy Loss Spectroscopy in the Electron Microscope* (Plenum Press, New York, 1986).

²See, for example, H. Raether, *Excitation of Plasmons and Interband Transitions by Electrons*, Springer Tracts in Modern Physics Vol. 88 (Springer-Verlag, New York, 1980).

³H. A. Bethe, *Ann. Phys. (Leipzig)* **5**, 325 (1930).

⁴P. M. Echenique and J. B. Pendry, *J. Phys. C* **8**, 2936 (1975).

⁵P. E. Batson, *Phys. Rev. Lett.* **49**, 936 (1982).

⁶C. Colliex, *Adv. Opt. Electron. Microsc.* **9**, 65 (1984).

⁷R. H. Ritchie and A. Howie, *Philos. Mag. A* **58**, 753 (1988).

⁸A. Howie and C. A. Walsh, *Radiat. Eff. Defects Solids* **117**, 169

(1991).

⁹C. A. Walsh, *Philos. Mag. A* **59**, 227 (1989).

¹⁰A. Howie and C. A. Walsh, *Microsc. Microanal. Microstruct.* **2**, 171 (1991).

¹¹R. G. Barrera and R. Fuchs, *Phys. Rev. B* **52**, 3256 (1995).

¹²R. Fuchs, R. G. Barrera, and J. L. Carrillo, *Phys. Rev. B* **54**, 12 824 (1996).

¹³K. Ghosh and R. Fuchs, *Phys. Rev. B* **44**, 7330 (1991); R. Fuchs and K. Ghosh, *Physica A* **207**, 185 (1994).

¹⁴D. A. G. Bruggeman, *Ann. Phys. (Leipzig)* **24**, 636 (1935).

¹⁵J. B. Pendry and L. Martín-Moreno, *Phys. Rev. B* **50**, 5062 (1994).